Supplementary Information for Extensive Quantum Chemistry Study of Neutral and Charged C_4N Chains. An Attempt to Aid Astronomical Observations

Ioan Bâldea*,†,‡

Theoretische Chemie, Universität Heidelberg, Im Neuenheimer Feld 229, D-69120 Heidelberg, Germany, and Institute of Space Sciences, National Institute of Lasers, Plasma and Radiation Physics, RO 077125, Bucharest-Măgurele, Romania

E-mail: ioan.baldea@pci.uni-heidelberg.de

*To whom correspondence should be addressed

†Theoretische Chemie, Universität Heidelberg, Im Neuenheimer Feld 229, D-69120 Heidelberg, Germany

‡Institute of Space Sciences, National Institute of Lasers, Plasma and Radiation Physics, RO 077125, Bucharest-Măgurele, Romania

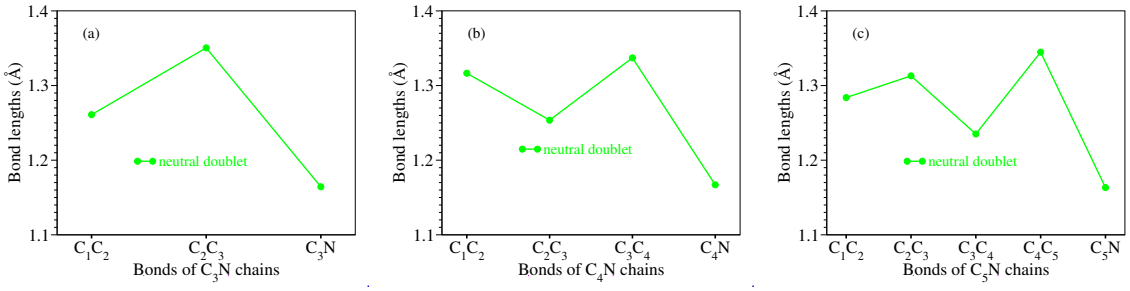

Figure S1: Bond lengths (in angstrom) of neutral C_4N, C_4N, and C_5N chains in their electronic ground state.

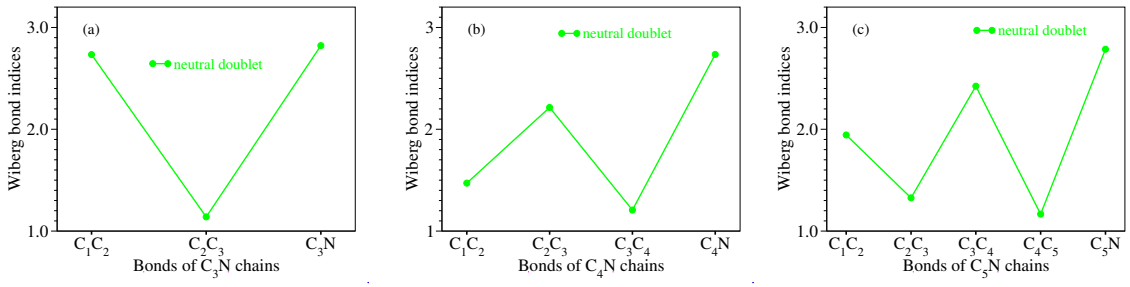

Figure S2: Wiberg bond indices of neutral C_4N, C_4N, and C_5N chains in their electronic ground state.

Table S1: Cartesian coordinates (in angstrom), natural charges and Wiberg valencies of the atoms of the (most stable) C_4N^0 neutral doublet ($\tilde{X}^2\Pi$).

Atom	X	Y	Z	charge	valence
C_1	0.000000	0.000000	2.65410363	0.27537	1.6424
C_2	0.000000	0.000000	1.33769693	-0.34620	3.8239
C_3	0.000000	0.000000	0.08416284	0.09058	3.6263
C_4	0.000000	0.000000	-1.25284849	0.17730	3.9745
N	0.000000	0.000000	-2.41981278	-0.19705	2.9459

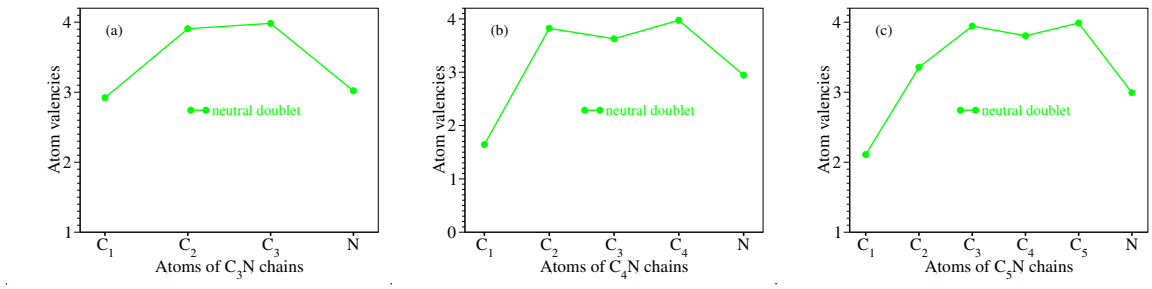

Figure S3: Wiberg valencies of neutral C_4N, C_4N, and C_5N chains in their electronic ground state.

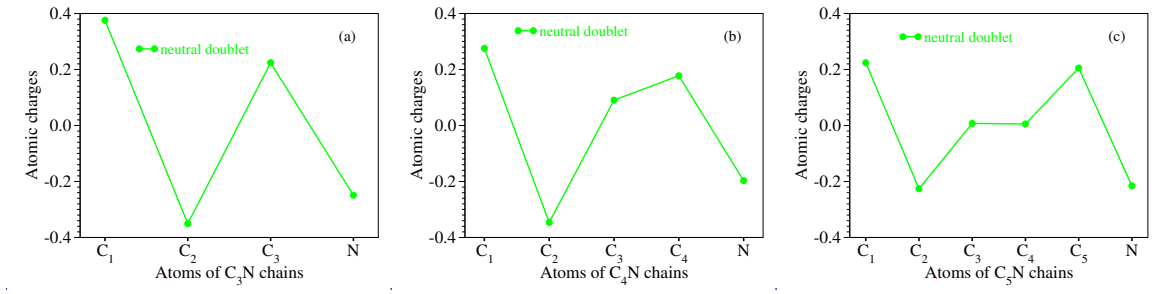

Figure S4: Atomic charges of neutral C_4N, C_4N, and C_5N chains in their electronic ground state.

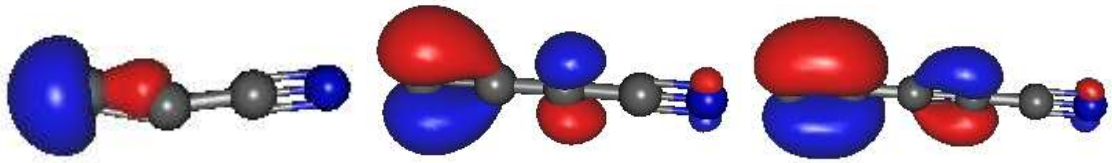

Figure S5: HOMO of neutral doublet C_3N^0, C_4N^0, and C_5N^0 chains.

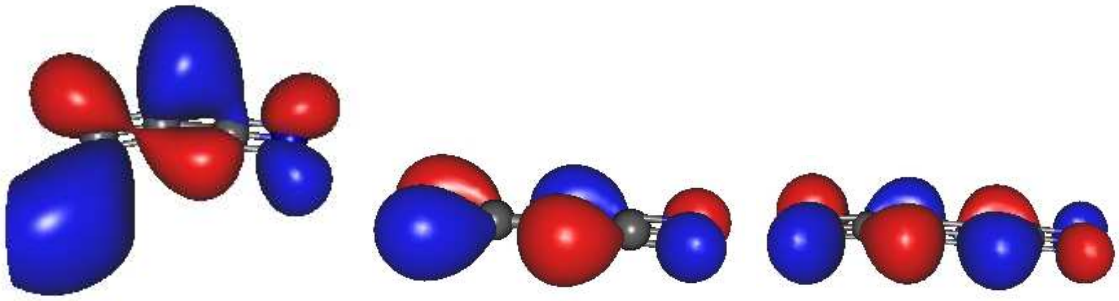

Figure S6: LUMO of neutral doublet C_3N^0, C_4N^0, and C_5N^0 chains.

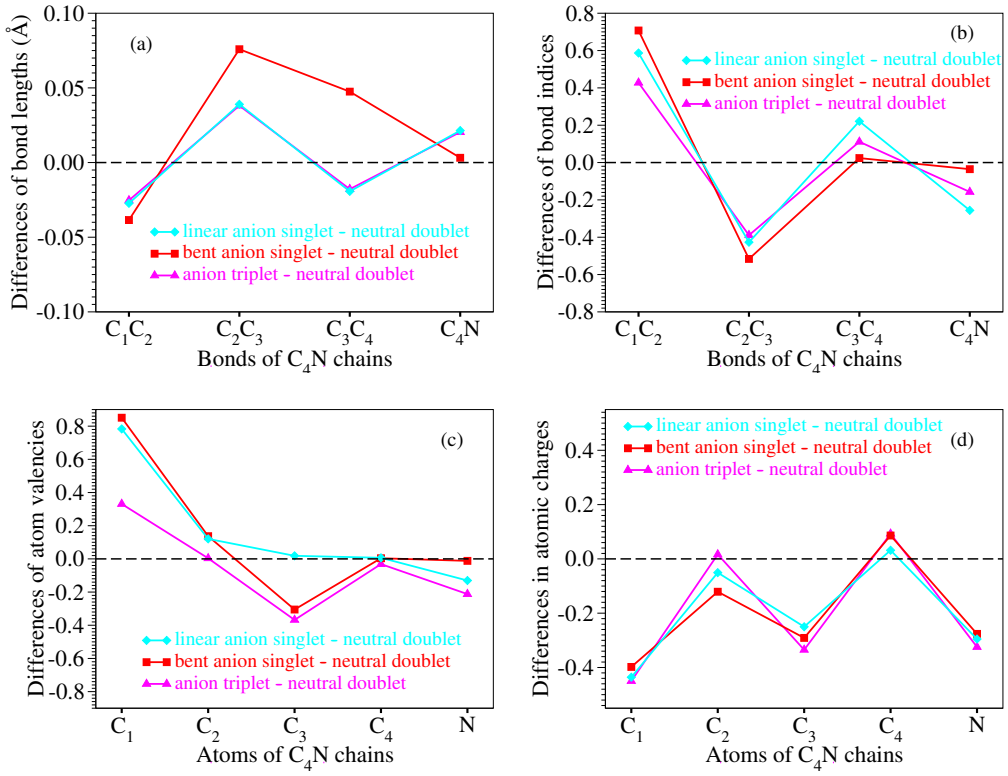

Figure S7: Changes with respect to the neutral doublet C_4N^0 of several molecular properties: (a) bond lengths (in angstrom), (b) Wiberg bond order indices, (c) Wiberg valencies and (d) atomic charges.

Table S2: Cartesian coordinates (in angstrom), natural charges and Wiberg valencies of the atoms of the (metastable) C_4N^0 neutral quartet ($\tilde{a}^4\Sigma^-$).

Atom	X	Y	Z	charge	valence
C_1	0.000000	0.000000	-2.61882889	0.38999	1.5361
C_2	0.000000	0.000000	-1.36043777	-0.25338	3.9155
C_3	0.000000	0.000000	-0.08294868	-0.08296	3.5336
C_4	0.000000	0.000000	1.24266035	0.21504	3.9845
N	0.000000	0.000000	2.41676142	-0.26869	2.9311

Table S3: Cartesian coordinates (in angstrom), natural charges and Wiberg valencies of the atoms of the (most stable) bent C_4N^- singlet ($^1A'$).

Atom	X	Y	Z	charge	valence
C_1	2.452143	-0.396162	0.000000	-0.12258	2.4933
C_2	1.261801	0.069056	0.000000	-0.46722	3.9608
C_3	0.078147	0.674522	0.000000	-0.20040	3.3211
C_4	-1.153197	0.041285	0.000000	0.26342	3.9784
N	-2.261910	-0.333173	0.000000	-0.47322	2.9340

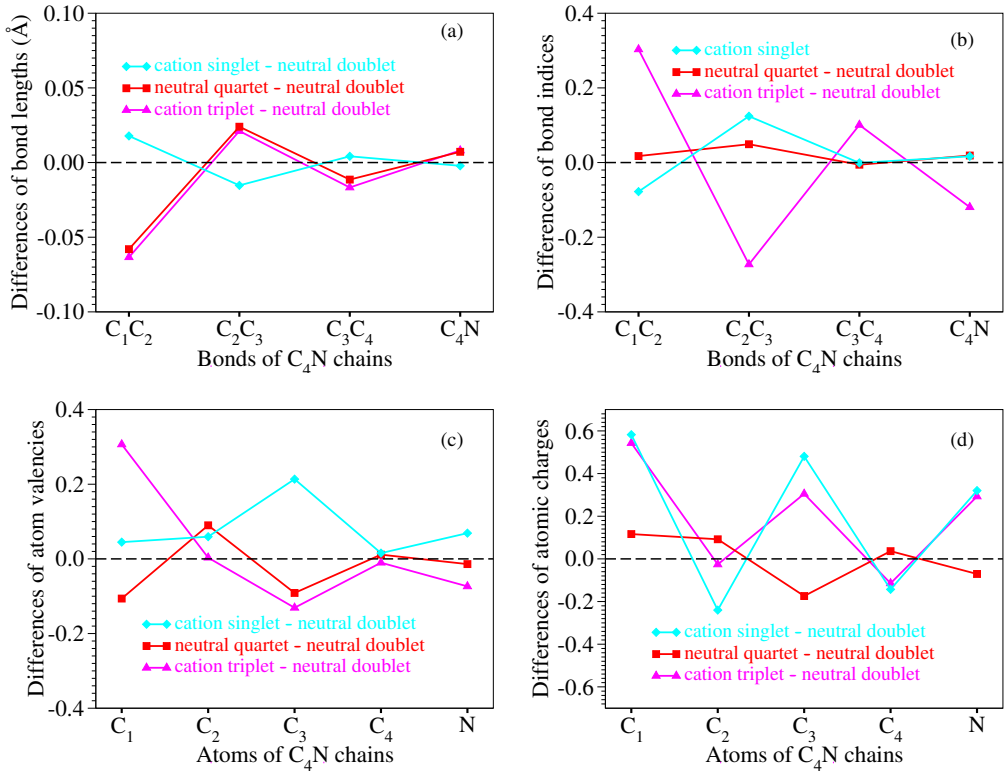

Figure S8: Changes with respect to the neutral doublet C_4N^0 of several molecular properties: (a) bond lengths (in angstrom), (b) Wiberg bond order indices, (c) Wiberg valencies and (d) atomic charges.

Table S4: Cartesian coordinates (in angstrom), natural charges and Wiberg valencies of the atoms of the (metastable, nearly) linear C_4N^- singlet ($^1\Sigma^-$).

Atom	X	Y	Z	charge	valence
C_1	5.057640	0.060822	0.000000	-0.16047	2.4257
C_2	3.768464	0.050142	0.000000	-0.39695	3.9445
C_3	2.475903	0.039685	0.000000	-0.15945	3.6447
C_4	1.158166	0.029423	0.000000	0.20914	3.9811
N	-0.030173	0.019929	0.000000	-0.49227	2.8156

Table S5: Cartesian coordinates (in angstrom), natural charges and Wiberg valencies of the atoms of the most stable linear C_4N^- triplet ($^3\Sigma^-$).

Atom	X	Y	Z	charge	valence
C_1	0.000000	0.000000	-2.65415168	-0.17449	1.9735
C_2	0.000000	0.000000	-1.36306952	-0.32969	3.8275
C_3	0.000000	0.000000	-0.07142727	-0.24430	3.2586
C_4	0.000000	0.000000	1.24775715	0.27001	3.9430
N	0.000000	0.000000	2.43504970	-0.52154	2.7338

Table S6: Cartesian coordinates (in angstrom), natural charges and Wiberg valencies of the atoms of the linear singlet C_4N^+ cation ($^1\Sigma^+$).

Atom	X	Y	Z	charge	valence
C_1	0.000000	0.000000	2.66019710	0.85764	1.6873
C_2	0.000000	0.000000	1.32621289	-0.58628	3.8834
C_3	0.000000	0.000000	0.08794830	0.57113	3.8399
C_4	0.000000	0.000000	-1.25330642	0.03453	3.9900
N	0.000000	0.000000	-2.41804446	0.12297	3.0149

Table S7: Cartesian coordinates (in angstrom), natural charges and Wiberg valencies of the atoms of the (metastable) linear triplet C_4N^+ cation ($^3\Sigma^+$).

Atom	X	Y	Z	charge	valence
C1	0.000000	0.000000	2.61065996	0.81831	1.9491
C2	0.000000	0.000000	1.35771105	-0.37213	3.8271
C3	0.000000	0.000000	0.08308407	0.39549	3.4954
C4	0.000000	0.000000	-1.23722188	0.06271	3.9643
N	0.000000	0.000000	-2.41219988	0.09561	2.8723

Table S8: Bond metric data for C_4N chains at geometries optimized using several exchange-correlation functionals and basis sets. Bond lengths l between atoms XY (in angstrom), angles α between atoms $\widehat{XYZ}$ (in degrees). Whenever angles between adjacent bonds are indicated, the geometries were optimized without imposing symmetry constraints.

Species	Method	Property	C_1C_2	$\widehat{C_1C_2C_3}$	C_2C_3	$\widehat{C_2C_3C_4}$	C_3C_4	$\widehat{C_3C_4N}$	C_4N
bent C_4N^- singlet	RB3LYP/6-311++G(3df, 3pd)	l, α	1.2780	174.3	1.3295	125.7	1.3846	171.4	1.1702
	RPBE0/6-311++G(3df, 3pd)		1.2792	174.3	1.3287	125.0	1.3847	171.6	1.1688
C_4N^- triplet	UB3LYP/6-311++G(3df, 3pd)	l, α	1.2912	179.8	1.2917	178.7	1.3193	180.0	1.1874
	UB3LYP/aug-cc-pVTZ		1.2913		1.2920		1.3197		1.1874
	UPBE0/6-311++G(3df, 3pd)		1.2938	179.8	1.2903	178.7	1.3209	180.0	1.1849
	UM06-2X/6-311++G(3df, 3pd)		1.2935		1.2877		1.3300		1.1774
	UB2GP-PLYP/6-311++G(3df, 3pd)		1.2924		1.2862		1.3293		1.1781
	ROCCSD(T)/aug-cc-PVTZ		1.3040		1.3027		1.3343		1.1944
C_4N^0 doublet	UB3LYP/6-311++G(3df, 3pd)	l, α	1.3165	179.8	1.2536	178.8	1.3371	180.0	1.1670
	UB3LYP/aug-cc-pVTZ		1.3169		1.2537		1.3377		1.1671
	UPBE0/6-311++G(3df, 3pd)		1.3193	179.8	1.2522	178.8	1.3386	180.0	1.1653
	UB2GP-PLYP/6-311++G(3df, 3pd)		1.3258		1.2330		1.3594		1.1539
	ROCCSD(T)/aug-cc-PVTZ		1.3357		1.2594		1.3581		1.1755
C_4N^0 quartet	UB3LYP/6-311++G(3df, 3pd)	l, α	1.2585	179.9	1.2776	178.8	1.3257	179.9	1.1742
	UB3LYP/aug-cc-pVTZ		1.2585		1.2777		1.3262		1.1742
	UPBE0/6-311++G(3df, 3pd)		1.2626		1.2735		1.3289		1.1717
C_4N^+ singlet	RB3LYP/6-311++G(3df, 3pd)	l, α	1.3343	178.8	1.2383	179.7	1.3413	179.6	1.1648
	RPBE0/6-311++G(3df, 3pd)		1.3361	178.7	1.2374	179.6	1.3421	179.7	1.1636
	B2GP-PLYP/6-311++G(3df, 3pd)		1.3326		1.2459		1.3407		1.1736
	RCCSD(T)/aug-cc-PVTZ		1.3343		1.2383		1.3413		1.1648
C_4N^+ triplet	UB3LYP/6-311++G(3df, 3pd)		1.2531	179.8	1.2747	178.9	1.3204	179.7	1.1751
	UPBE0/6-311++G(3df, 3pd)		1.2564		1.2722		1.3216		1.1737

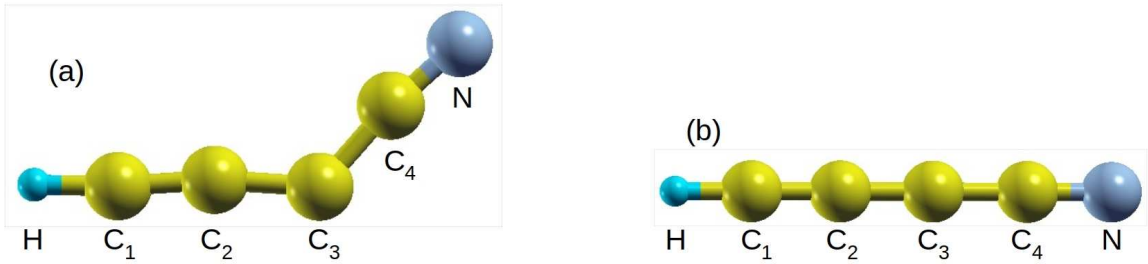

Figure S9: Geometries of singlet and triplet HC_4N chains (left and right panels, respectively) investigated in the present paper.

Table S9: Natural charges and Wiberg valencies of the atoms of the bent stable HC_4N (second and third columns) and C_4N^- (fourth and fifth columns) singlets.

Atom	charge	valence	charge	valence
H	0.23992	0.9448	—	—
C_1	-0.02018	3.6818	-0.12258	2.4933
C_2	-0.19260	3.9373	-0.46722	3.9608
C_3	0.06473	3.0972	-0.20040	3.3211
C_4	0.15035	3.9731	0.26342	3.9784
N	-0.24222	2.9193	-0.47322	2.9340

Table S10: Natural charges and Wiberg valencies of the atoms of the stable HC_4N (second and third columns) and C_4N^- (fourth and fifth columns) triplets.

Atom	charge	valence	charge	valence
H	0.24010	0.9448	—	—
C_1	-0.06097	3.4399	-0.17449	1.9735
C_2	-0.21113	3.9731	-0.32969	3.8275
C_3	0.16184	2.8127	-0.24430	3.2586
C_4	0.14022	3.9897	0.27001	3.9430
N	-0.27006	2.7173	-0.52154	2.7338

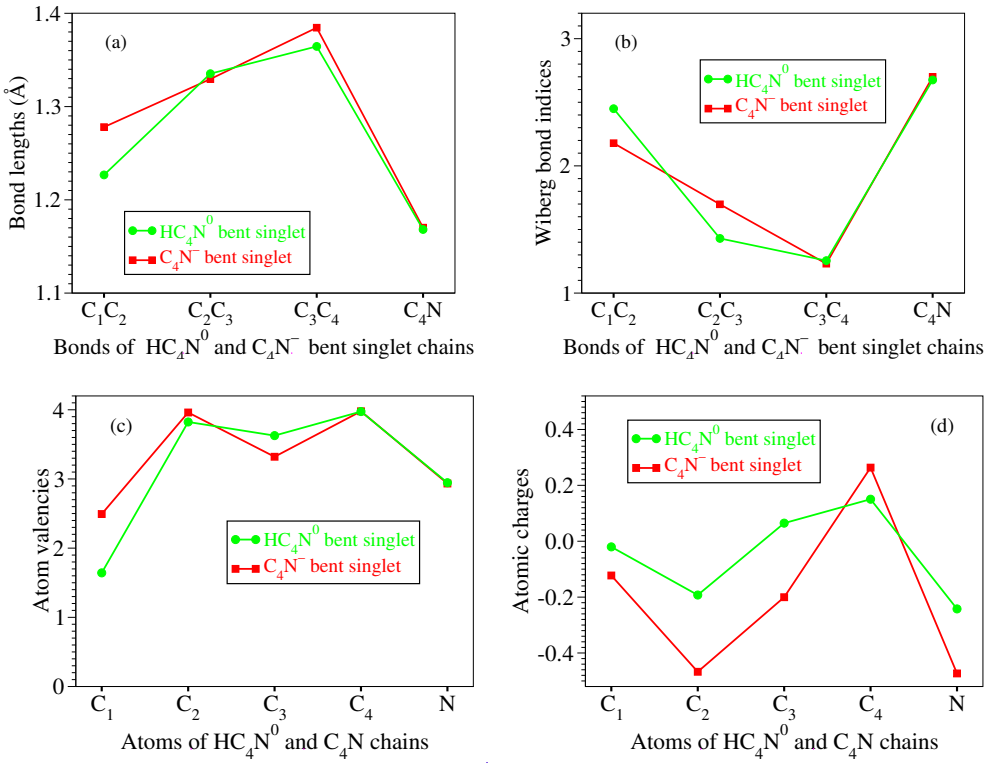

Figure S10: (a) Bond lengths (in angstrom), (b) Wiberg bond indices, (c) Wiberg valencies and (d) atomic charges of the isoelectronic HC_4N and C_4N^- singlet bent chains considered in this paper.

Table S11: Values of the vertical and adiabatic doublet-quartet splitting ($\Delta^0_{DQ}\left(\mathbf{R}^0_{D,Q}\right) \equiv \mathcal{E}^0_Q\left(\mathbf{R}^0_{D,Q}\right) - \mathcal{E}^0_{DE}\left(\mathbf{R}^0_{D,Q}\right)$ and $\Delta^{ad}_{DQ} \equiv \mathcal{E}^0_Q\left(\mathbf{R}^0_Q\right) - \mathcal{E}^0_D\left(\mathbf{R}^0_D\right)$, respectively) computed without and with corrections due to zero point motion at geometries ($\mathbf{R}^0_x, x = D, Q$) optimized using the largest Pople basis sets 6-311++G(3df, 3pd) and several exchange-correlation functionals.

		B3LYP	PBE0	M06-2X
$\Delta^0_{DQ}\left(\mathbf{R}^0_D\right)$	uncorrected	1.167	0.921	0.979
	corrected	1.182	0.946	0.971
$\Delta^0_{DQ}\left(\mathbf{R}^0_Q\right)$	uncorrected	1.062	0.742	0.777
	corrected	1.076	0.766	0.770
$\Delta^{0,ad}_{DQ}$	uncorrected	1.167	0.839	0.889
	corrected	1.182	0.864	0.881

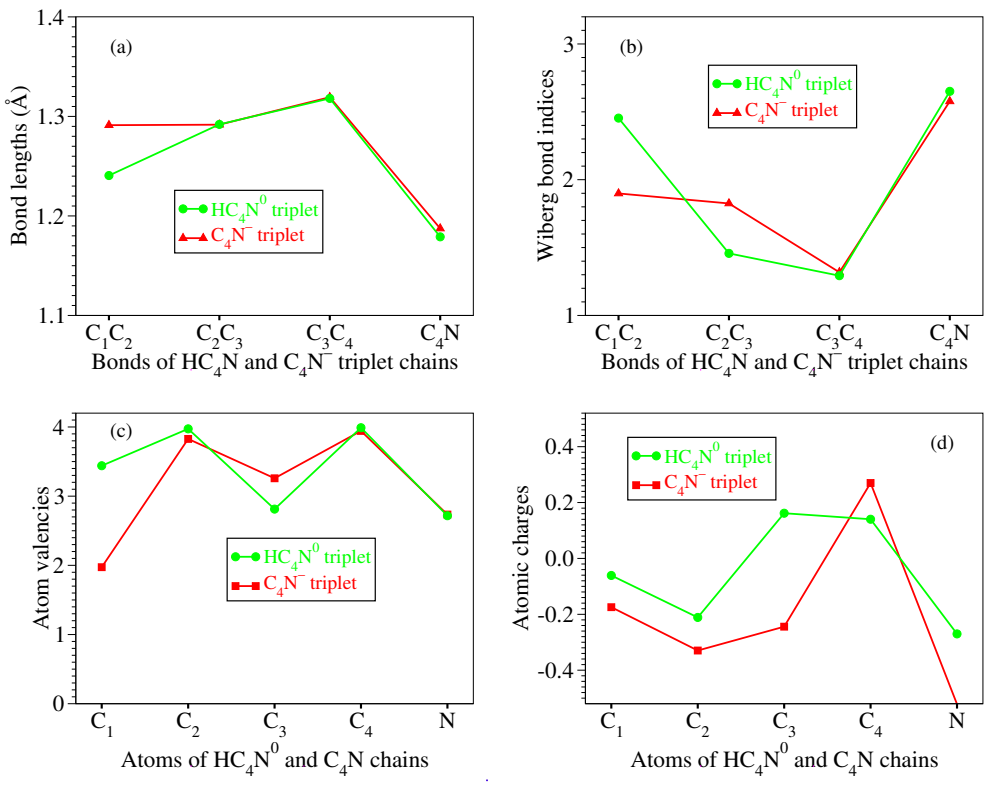

Figure S11: (a) Bond lengths (in angstrom), (b) Wiberg bond indices, (c) Wiberg valencies and (d) atomic charges of HC_4N and C_4N^- triplet chains considered in this paper.

Table S12: Values of the vertical ($\Delta^-_{bS,T}\left(\mathbf{R}^-_T\right) \equiv \mathcal{E}^-_T\left(\mathbf{R}^-_T\right) - \mathcal{E}^-_{bS}\left(\mathbf{R}^-_T\right)$ $\Delta^-_{bS,T}\left(\mathbf{R}^-_{bS}\right) \equiv \mathcal{E}^-_T\left(\mathbf{R}^-_{bS}\right) - \mathcal{E}^-_{bS}\left(\mathbf{R}^-_{bS}\right)$ $\Delta^-_{lS,T}\left(\mathbf{R}^-_{lS}\right) \equiv \mathcal{E}^-_T\left(\mathbf{R}^-_{lS}\right) - \mathcal{E}^-_{lS}\left(\mathbf{R}^-_{lS}\right)$) and adiabatic singlet-triplet splitting computed without and with corrections due to zero point motion using geometries ($\mathbf{R}^-_x, x = T, bS, lS$) optimized using the largest Pople basis sets 6-311++G(3df, 3pd) and several exchange-correlation functionals.

		B3LYP	PBE0	M06-2X
$-\Delta^-_{bS,T}\left(\mathbf{R}^-_T\right)$	uncorrected	0.785	0.917	0.615
	corrected	0.791	0.923	0.615
$-\Delta^-_{bS,T}\left(\mathbf{R}^-_{bS}\right)$	uncorrected	0.103	0.224	-0.013
	corrected	0.109	0.230	-0.013
$-\Delta^{-,ad}_{bS,T}$	uncorrected	0.527	0.661	0.503
	corrected	0.533	0.667	0.503

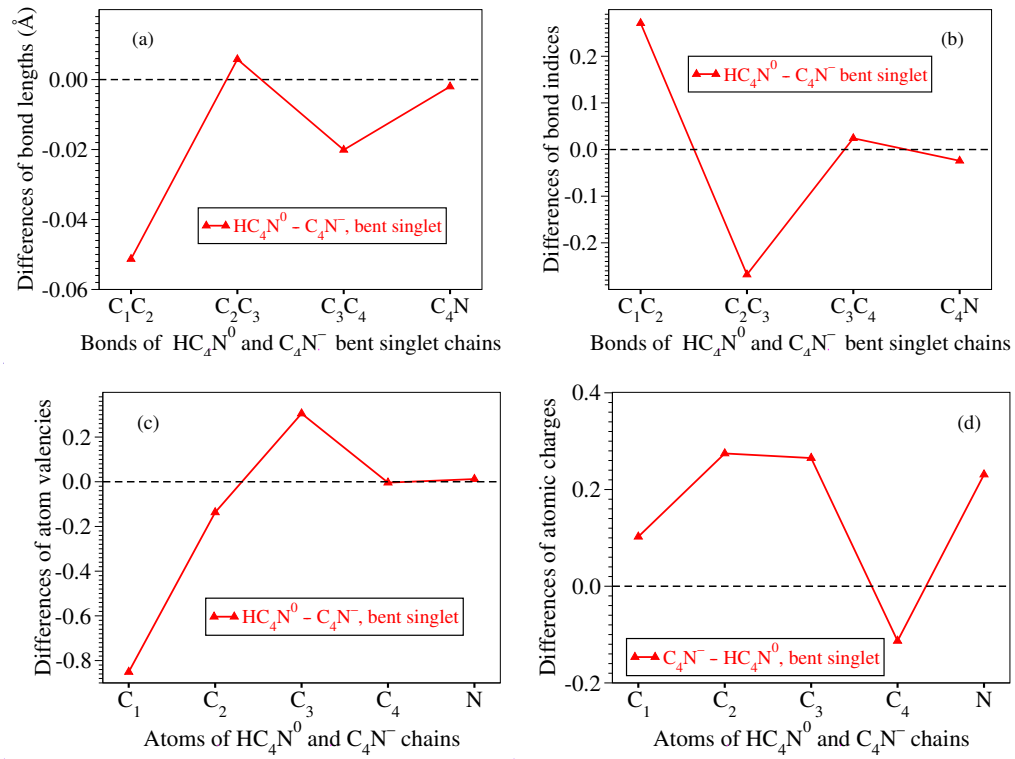

Figure S12: Differences between several molecular properties of the isoelectronic HC_4N and C_4N^- singlet bent chains considered in this paper: (a) bond lengths (in angstrom), (b) Wiberg bond indices, (c) Wiberg valencies and (d) atomic charges.

Table S13: Values of adiabatic anion singlet-triplet splittings obtained within unrestricted ab initio methods with zero-point motion corrections. Values in italics are deduced from Pascoli and Lavendy[19].

Method	Basis set	$-\Delta^{-,ad}_{T,bS}$	$-\Delta^{-,ad}_{T,lS}$
B3LYP	6-311G*	*0.57*	*0.81*
B3LYP	aug-cc-pVTZ	*0.53*	*0.78*
B3LYP	6-311++G(3df, 3pd)	0.533	0.791
QCISD	6-311G*	*0.40*	*0.87*
QCISD	6-311++G(3df, 3pd)	0.374	0.824
QCISD(T)	6-311G*	*0.27*	*0.72*
QCISD(T)	6-311++G(3df, 3pd)	0.243	0.671
CCSD	6-311G*	*0.39*	*0.87*
CCSD	6-311++G(3df, 3pd)	0.367	0.822
CCSD(T)	6-311G*	*0.25*	*0.71*
CCSD(T)	6-311++G(3df, 3pd)	0.234	0.653

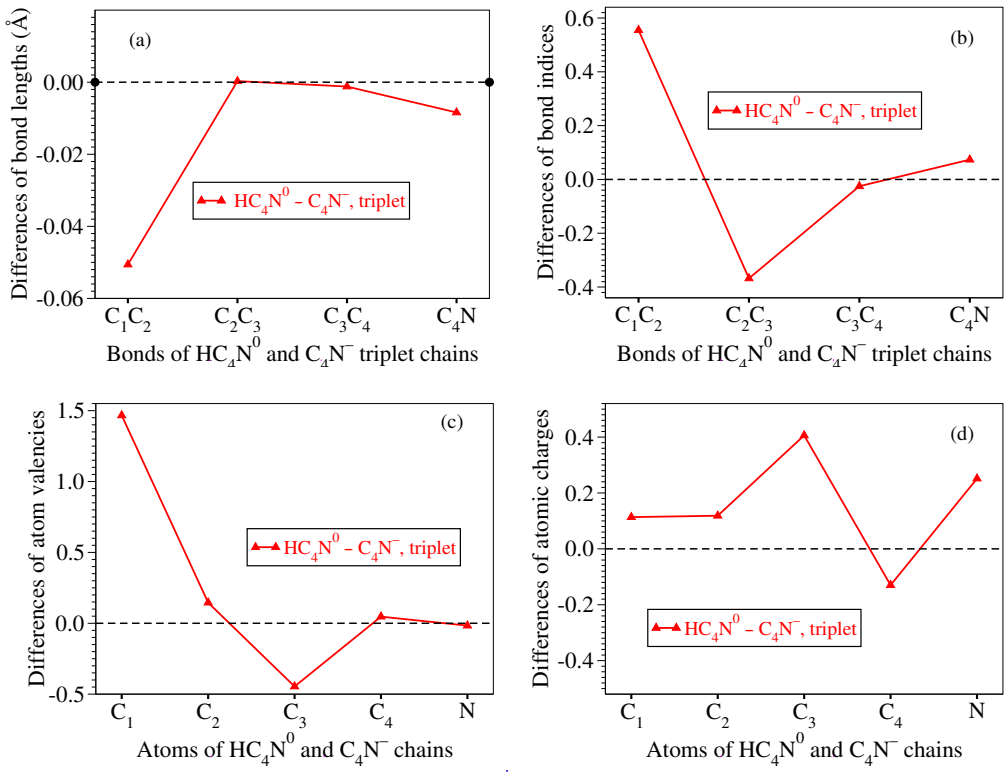

Figure S13: Differences between several molecular properties of the isoelectronic HC_4N and C_4N^- linear triplet chains considered in this paper: (a) bond lengths (in angstrom), (b) Wiberg bond indices, (c) Wiberg valencies and (d) atomic charges.

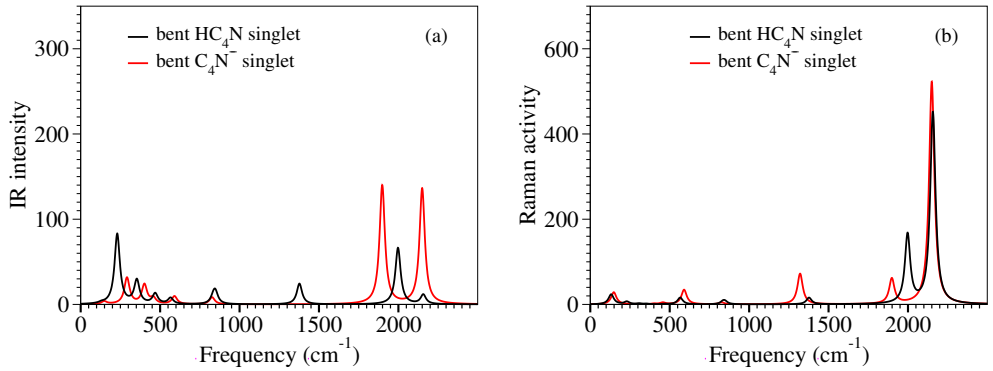

Figure S14: (a) Infrared and (b) Raman spectra of HC_4N and C_4N^- bent singlet chains considered in this paper.

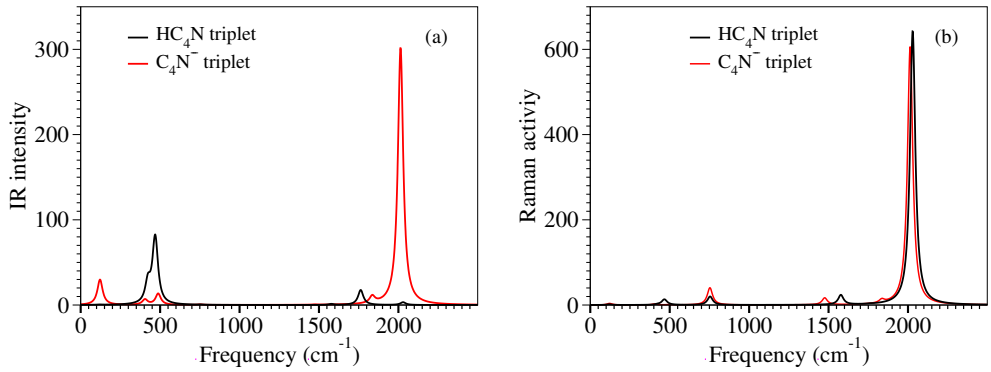

Figure S15: (a) Infrared and (b) Raman spectra of HC_4N and C_4N^- triplet chains considered in this paper.

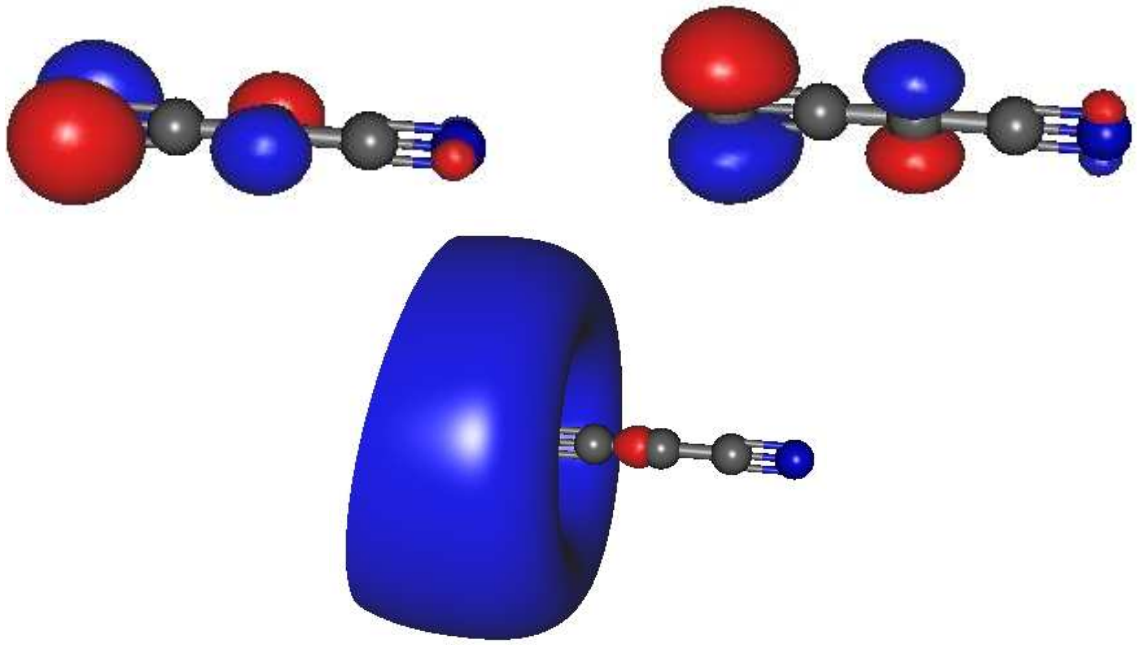

Figure S16: Degenerate HOMO and HOMO-1 (upper left and right panel, respectively) and LUMO (lower panel) of the neutral C_4N^0 quartet ($\tilde{a}^4\Sigma^-$).

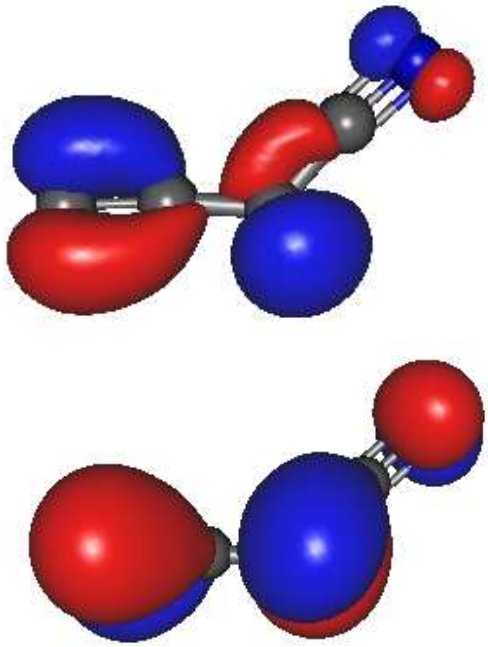

Figure S17: HOMO and LUMO (upper and lower panel, respectively) of the bent C_4N^- singlet ($^1A'$).

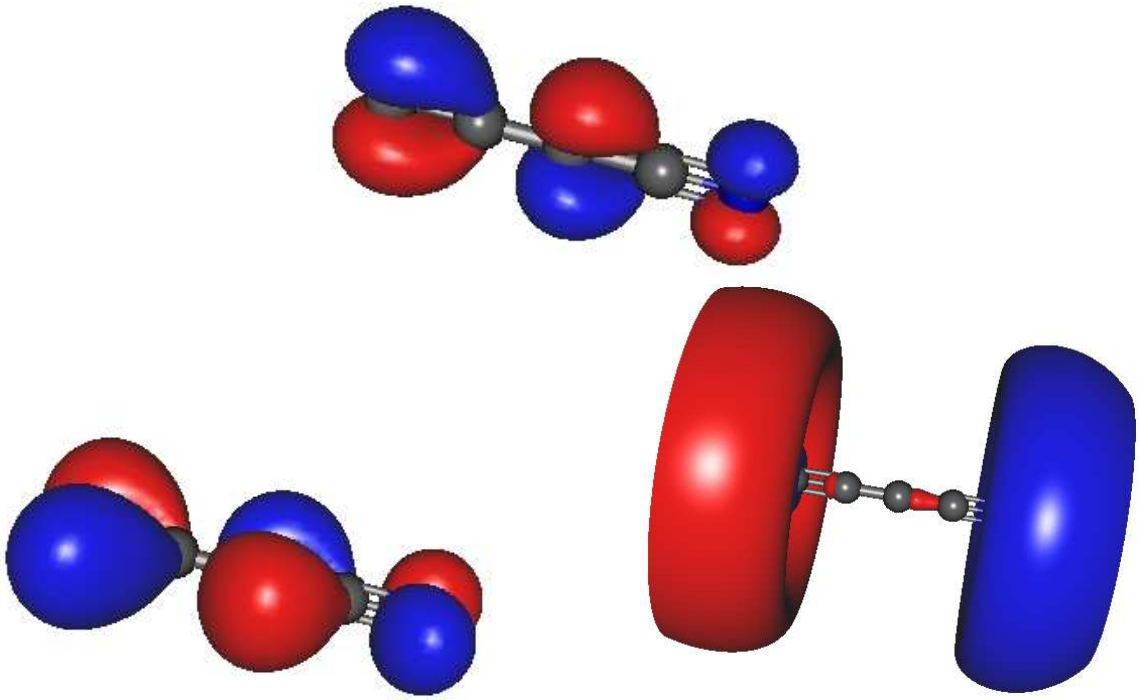

Figure S18: HOMO (upper panel) and nearly degenerate LUMO and LUMO+1 (lower left and right panel, respectively) of the linear C_4N^- singlet ($^1\Sigma^-$).

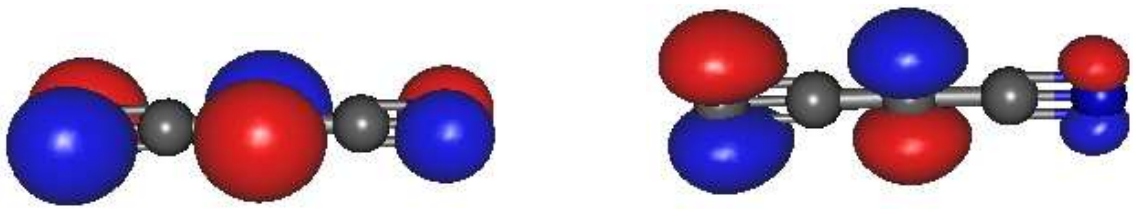

Figure S19: HOMO and LUMO (left and right panel, respectively) of the C_4N^+ triplet ($^3\Sigma^+$).

Table S14: Values of vertical and adiabatic cation singlet-triplet splitting ($\Delta_{ST}^{+}\left(\mathbf{R}_{S,T}^{+}\right) \equiv \mathcal{E}_T^{+}\left(\mathbf{R}_{S,T}^{+}\right) - \mathcal{E}_S^{+}\left(\mathbf{R}_{S,T}^{+}\right)$) and $\Delta_{ST}^{+,ad} \equiv \mathcal{E}_T^{+}\left(\mathbf{R}_{T}^{+}\right) - \mathcal{E}_S^{+}\left(\mathbf{R}_{S}^{+}\right)$, respectively) computed without and with corrections due to zero point motion with geometries $\mathbf{R}_{S,T}^{+}$ optimized using several exchange-correlation functionals and 6-311++G(3df, 3pd) basis sets.

		B3LYP	PBE0	M06-2X
$\Delta_{ST}^{+}\left(\mathbf{R}_{S}^{+}\right)$	uncorrected	1.517	1.250	1.451
	corrected	1.489	1.251	1.441
$\Delta_{ST}^{+}\left(\mathbf{R}_{T}^{+}\right)$	uncorrected	1.046	0.796	0.965
	corrected	1.018	0.797	0.955
$\Delta_{ST}^{+,ad}$	uncorrected	1.311	1.052	1.247
	corrected	1.283	1.054	1.236

Table S15: Longitudinal (nonvanishing A only for bent anion singlet) and perpendicular ($B = C$ except for the bent anion singlet) rotational constants of the C_4N chains investigated in this paper computed by using methods indicated in the second column.

Species	Method	A (GHz)	B (GHz)	C (GHz)
neutral doublet	UB3LYP/6-311++G(3df, 3pd)		2.44239	
	UPBE0/6-311++G(3df, 3pd)		2.44128	
	UM06-2X/6-311++G(3df, 3pd)		2.43646	
	UB2GP-PLYP/6-311++G(3df, 3pd)		2.44310	
	UHF/3-21G[14]		2.4075	
	UHF/svp[14]		2.3963	
neutral quartet	UB3LYP/6-311++G(3df, 3pd)		2.46635	
	UPBE0/6-311++G(3df, 3pd)		2.46586	
	UM06-2X/6-311++G(3df, 3pd)		2.46171	
anion triplet	UB3LYP/6-311++G(3df, 3pd)		2.42267	
	UPBE0/6-311++G(3df, 3pd)		2.42220	
	UM06-2X/6-311++G(3df, 3pd)		2.42084	
	UB2GP-PLYP/6-311++G(3df, 3pd)		2.42361	
bent anion singlet	RB3LYP/6-311++G(3df, 3pd)	56.30860	2.82435	2.68945
	RPBE0/6-311++G(3df, 3pd)	54.50451	2.84356	2.70256
	RM06-2X/6-311++G(3df, 3pd)	46.19743	2.92536	2.75115
cation singlet	RB3LYP/6-311++G(3df, 3pd)		2.44330	
	RPBE0/6-311++G(3df, 3pd)		2.44262	
	RM06-2X/6-311++G(3df, 3pd)		2.44031	
	RB2GP-PLYP/6-311++G(3df, 3pd)		2.42933	
cation triplet	UB3LYP/6-311++G		2.47931	
	UPBE0/6-311++G		2.47907	
	UM06-2X/6-311++G(3df, 3pd)		2.47802	

Table S16: Values of the dipole momentum **D** (field independent basis, debye) at various levels of theory indicated in the second column. Notice that the value in italics obtained by Pauzat *et al.*[14] within the UHF/svp approach is somewhat different from that of our calculations at the same level of theory.

Species	Method	D_X	D_Y	D_Z	D_{total}
neutral doublet	B3LYP/6-311++G(3df, 3pd)	0.0000	0.0000	0.3347	0.3347
	B3LYP/aug-cc-pVTZ	0.0000	0.0000	0.3393	0.3393
	UCCSD(T)/6-311++G(3df, 3pd)	0.0000	0.0000	0.0907	0.0907
	UCCSD(T)/aug-cc-pvtz	0.0000	0.0000	0.0990	0.0990
	ROCCSD(T)/6-311++G(3df, 3pd)	0.0000	0.0000	0.4512	0.4512
	ROCCSD(T)/aug-cc-pVTZ	0.0000	0.0000	0.4436	0.4436
	UHF/3-21g	0.0000	0.0000	0.0544	0.0544
	UHF/svp	0.0000	0.0000	0.1119	0.1119
	UHF/svp[14]	0.0000	0.0000	*0.14*	*0.14*
	UHF/6-311++G(3df, 3pd)	0.0000	0.0000	0.0587	0.0587
	UHF/aug-cc-pvtz	0.0000	0.0000	0.0654	0.0654
	ROHF/3-21g	0.0000	0.0000	0.5486	0.5486
	ROHF/svp	0.0000	0.0000	0.6216	0.6216
	ROHF/6-311++G(3df, 3pd)	0.0000	0.0000	0.7821	0.7821
	ROHF/aug-cc-pVTZ	0.0000	0.0000	0.7781	0.7781
neutral quartet	B3LYP/6-311++G(3df, 3pd)	0.0000	0.0000	3.4628	3.4628
	B3LYP/aug-cc-pVTZ	0.0000	0.0000	3.4586	3.4586
	UCCSD(T)/6-311++G(3df, 3pd)	0.0000	0.0000	3.2558	3.2558
	ROCCSD(T)/6-311++G(3df, 3pd)	0.0000	0.0000	4.5003	4.5003
	ROCCSD(T)/aug-cc-pVTZ	0.0000	0.0000	4.4940	4.4940
	UHF/3-21G	0.0000	0.0000	2.9749	2.9749
	UHF/svp	0.0000	0.0000	3.1581	3.1581
	UHF/6-311++G(3df, 3pd)	0.0000	0.0000	3.2558	3.2558
	UHF/aug-ccpVTZ	0.0000	0.0000	3.2479	3.2479
	ROHF/3-21G	0.0000	0.0000	3.8729	3.8729
	ROHF/svp	0.0000	0.0000	4.2865	4.2865
	ROHF/6-31++G(3df, 3pd)	0.0000	0.0000	4.5003	4.5003
	ROHF/aug-cc-pvtz	0.0000	0.0000	4.4940	4.4940
anion triplet	B3LYP/6-311++G(3df, 3pd)	0.0000	0.0000	2.9398	2.9398
	B3LYP/aug-cc-pVTZ	0.0000	0.0000	2.9340	2.9400
	UCCSD(T)/6-311++G(3df, 3pd)	0.0000	0.0000	4.4930	4.4930
	ROCCSD(T)/6-311++G(3df, 3pd)	0.0000	0.0000	2.2379	2.2379
	ROCCSD(T)/aug-cc-pVTZ	0.0000	0.0000	2.2447	2.2447
	UHF/3-21G	0.0000	0.0000	4.5640	4.5640
	UHF/svp	0.0000	0.0000	4.4277	4.4277
	UHF/6-311++G(3df, 3pd)	0.0000	0.0000	4.4930	4.4930
	UHF/aug-cc-pVTZ	0.0000	0.0000	4.5002	4.5002
	ROHF/3-21G	0.0000	0.0000	2.4519	2.4519
	ROHF/svp	0.0000	0.0000	2.3422	2.3422
	ROHF/6-311++G(3df, 3pd)	0.0000	0.0000	2.2379	2.2379
	ROHF/aug-cc-pVTZ	0.0000	0.0000	2.5956	2.5956

Table S17: Values of the quadrupole momentum **Q** (field independent basis, debye-angstrom) of the C_4N chains investigated in this paper obtained using geometries optimized as indicated in the second column.

Species	Method	Q_{xx}	Q_{yy}	Q_{zz}	Q_{xy}	Q_{xz}	Q_{yz}
neutral doublet	B3LYP/6-311++G(3df, 3pd)	-26.3541	-27.9983	-42.2421	0.0000	0.0000	0.0000
	B3LYP/aug-cc-pVTZ	-26.3443	-27.9421	-42.2635	0.0000	0.0000	0.0000
	UCCSD(T)/6-311++G(3df, 3pd)	-26.4146	-28.2057	-42.2981	0.0000	0.0000	0.0000
	UCCSD(T)/aug-cc-pvtz	-26.3955	-28.1379	-42.3180	0.0000	0.0000	0.0000
	ROCCSD(T)/6-311++G(3df, 3pd)	-28.4353	-26.8169	-41.6984	0.0000	0.0000	0.0000
	ROCCSD(T)/aug-cc-pVTZ	-26.8005	-28.3699	-41.7230	0.0000	0.0000	0.0000
	UHF/3-21g	-28.2685	-26.4478	-41.7598	0.0000	0.0000	0.0000
	UHF/svp	-26.5232	-28.3367	-42.6564	0.0000	0.0000	0.0000
	UHF/6-311++G(3df, 3pd)	-26.4489	-28.2494	-42.2687	0.0000	0.0000	0.0000
	UHF/aug-cc-pvtz	-28.1845	-26.4327	-42.2852	0.0000	0.0000	0.0000
neutral quartet	B3LYP/6-311++G(3df, 3pd)	-27.5520	-27.5520	-30.7287	0.0000	0.0000	0.0000
	B3LYP/aug-cc-pVTZ	-27.5250	-27.5250	-30.7352	0.0000	0.0000	0.0000
	UCCSD(T)/6-311++G(3df, 3pd)	-27.6065	-27.6065	-30.5244	0.0000	0.0000	0.0000
	ROCCSD(T)/6-311++G(3df, 3pd)	-28.0387	-28.0387	-29.5375	0.0000	0.0000	0.0000
	ROCCSD(T)/aug-cc-pVTZ	-27.9995	-27.9995	-29.5470	0.0000	0.0000	0.0000
anion triplet	B3LYP/6-311++G(3df, 3pd)	-31.7023	-31.7023	-71.4631	0.0000	0.0000	0.0000
	B3LYP/aug-cc-pVTZ	-31.6879	-31.6879	-71.5144	0.0000	0.0000	0.0000
	UCCSD(T)/6-311++G(3df, 3pd)	-31.8018	-31.8018	-71.7508	0.0000	0.0000	0.0000
	ROCCSD(T)/6-311++G(3df, 3pd)	-32.1142	-32.1142	-70.2281	0.0000	0.0000	0.0000
	ROCCSD(T)/aug-cc-pVTZ	-32.0834	-32.0834	-70.2791	0.0000	0.0000	0.0000
bent anion singlet	B3LYP/6-311++G(3df, 3pd)	-63.8640	-36.8339	-30.3058	1.4754	0.0000	0.0000
	B3LYP/aug-cc-pVTZ	-63.8640	-36.8339	-30.3058	1.4754	0.0000	0.0000
	RCCSD(T)/6-311++G(3df, 3pd)	-62.9911	-37.1863	-30.6481	1.1594	0.0000	0.0000
	RCCSD(T)/aug-cc-pVTZ	-63.0000	-37.1600	-30.6336	1.1690	0.0000	0.0000
linear anion singlet	B3LYP/6-311++G(3df, 3pd)	-29.8650	-33.8601	-71.3765	0.0000	0.0000	0.0000
	B3LYP/aug-cc-pVTZ	-29.9174	-33.8018	-71.4570	0.0000	0.0000	0.0000
	RCCSD(T)/6-311++G(3df, 3pd)	-30.2092	-34.2094	-70.3492	0.0000	0.0000	0.0000
	RCCSD(T)/aug-cc-pVTZ	-34.1124	-30.2533	-70.4022	0.0000	0.0000	0.0000
cation singlet	B3LYP/6-311++G(3df, 3pd)	-23.7770	-23.7770	-15.6956	0.0000	0.0000	0.0000
	B3LYP/aug-cc-pVTZ	-23.7770	-23.7770	-15.6957	0.0000	0.0000	0.0000
	RCCSD(T)/6-311++G(3df, 3pd)	-23.7366	-23.7366	-15.7048	0.0000	0.0000	0.0000
	RCCSD(T)/aug-cc-pVTZ	-24.3542	-24.3542	-14.1423	0.0000	0.0000	0.0000
cation triplet	B3LYP/6-311++G(3df, 3pd)	-23.4092	-24.8186	-6.0974	0.0000	0.0000	0.0000
	B3LYP/aug-cc-pVTZ	-24.7575	-23.3930	-6.1030	0.0000	0.0000	0.0000
	UCCSD(T)/6-311++G(3df, 3pd)	-25.0731	-23.7379	-7.4195	0.0000	0.0000	0.0000
	ROCCSD(T)/6-311++G(3df, 3pd)	-24.0058	-25.3116	-5.2179	0.0000	0.0000	0.0000
	ROCCSD(T)/aug-cc-pVTZ	-25.2346	-23.9786	-5.2274	0.0000	0.0000	0.0000

Table S18: Values of the higher vibrational frequencies (in cm^{-1}) of the presently investigated molecular species obtained via B3LYP/6-311++G(3df, 3pd) calculations.

Description	C_4N^0 doublet	C_4N^0 quartet bent	C_4N^- singlet	C_4N^- triplet	C_4N^+ singlet	C_4N^+ triplet	HC_4N singlet	HC_4N triplet
symmetric stretch (breath.)	752.62	765.66	827.08	753.17	756.09	775.07	847.97	754.26
out-of-phase C_1C_2—C_4N stretch	1421.85	1559.49	1320.77	1475.77	1418.37	1579.14	1376.99	1577.41
in-phase C_1C_2—C_4N stretch	1989.43	1753.86	1898.25	1835.45	2198.39	1956.48	1997.43	1762.66
CN stretch	2181.87	2071.92	2149.62	2013.49	2325.12	2138.33	2156.55	2029.44
CH stretch	—	—	—	—	—	—	3449.65	3446.77

Table S19: Values of the vertical and adiabatic doublet-triplet electron attachment energies ($EA_{TD}^{vert}(\mathbf{R}) \equiv \mathcal{E}_D^0(\mathbf{R}) - \mathcal{E}_T^-(\mathbf{R})$ and $EA_{TD}^{ad} \equiv \mathcal{E}_D^0(\mathbf{R}_D^0) - \mathcal{E}_T^-(\mathbf{R}_T^-)$, respectively) computed without and with corrections due to zero point motion using the neutral doublet ($\mathbf{R} = \mathbf{R}_D^0$) and anion triplet ($\mathbf{R} = \mathbf{R}_T^-$) B3LYP/6-311++G(3df, 3pd) optimum geometries.

		EOM-ROCCSD	B3LYP	LC-BLYP	LC-ωPBE
$EA_{TD}^{vert}(\mathbf{R}_D^0)$	uncorrected	3.027	3.217	3.479	3.514
	corrected	3.017	3.207	3.469	3.504
$EA_{TD}^{vert}(\mathbf{R}_T^-)$	uncorrected	3.199	3.360	3.670	3.690
	corrected	3.189	3.350	3.659	3.679
EA_{TD}^{ad}	uncorrected	3.109	3.285	3.497	3.545
	corrected	3.099	3.274	3.486	3.534

Table S20: Values of the vertical and adiabatic doublet-triplet electron attachment energies ($EA_{TD}^{vert}(\mathbf{R}) \equiv \mathcal{E}_D^0(\mathbf{R}) - \mathcal{E}_T^-(\mathbf{R})$ and $EA_{TD}^{ad} \equiv \mathcal{E}_D^0(\mathbf{R}_D^0) - \mathcal{E}_T^-(\mathbf{R}_T^-)$, respectively) computed without and with corrections due to zero point motion using the neutral doublet $\mathbf{R}_D^0$ and anion triplet $\mathbf{R}_T^-$ geometries optimized within B3LYP/6-311++G(3df, 3pd) and PBE0/6-311++G(3df, 3pd).

		B3LYP	PBE0	EOM-ROCCSD@B3LYP	EOM-ROCCSD@PBE0
$EA_{TD}^{vert}(\mathbf{R}_D^0)$	uncorrected	3.217	3.288	3.027	3.006
	corrected	3.207	3.275	3.017	2.993
$EA_{TD}^{vert}(\mathbf{R}_T^-)$	uncorrected	3.360	3.431	3.199	3.175
	corrected	3.350	3.418	3.189	3.162
EA_{TD}^{ad}	uncorrected	3.285	3.355	3.109	3.086
	corrected	3.274	3.342	3.099	3.073

Table S21: Values of the vertical and adiabatic doublet-triplet electron attachment EA computed without and with corrections due to zero point motion using the neutral doublet $\mathbf{R}_D^0$ and anion triplet $\mathbf{R}_T^-$ geometries optimized by means of several functionals and 6-311++G(3df, 3pd) basis sets.

		B3LYP	PBE0	M06-2X
$EA_{TD}^{vert}\left(\mathbf{R}_D^0\right)$	uncorrected	3.217	3.288	3.304
	corrected	3.207	3.275	3.317
$EA_{TD}^{vert}\left(\mathbf{R}_T^-\right)$	uncorrected	3.360	3.431	3.273
	corrected	3.350	3.418	3.285
EA_{TD}^{ad}	uncorrected	3.285	3.355	3.386
	corrected	3.274	3.342	3.398

Table S22: Values of the vertical and adiabatic doublet-singlet ionization energy ($IP_{SD}^{vert}\left(\mathbf{R}\right) \equiv \mathcal{E}_S^+\left(\mathbf{R}\right) - \mathcal{E}_D^0\left(\mathbf{R}\right)$ and $IP_{SD}^{ad} \equiv \mathcal{E}_S^+\left(\mathbf{R}_S^+\right) - \mathcal{E}_D^0\left(\mathbf{R}_D^0\right)$, respectively) computed without and with with corrections due to zero point motion using the neutral doublet ($\mathbf{R} = \mathbf{R}_D^0$) and cation singlet ($\mathbf{R} = \mathbf{R}_S^+$) B3LYP/6-311++G(3df, 3pd) optimum geometries.

		EOM-ROCCSD	B3LYP	LC-BLYP	LC-ωPBE
$IP_{SD}^{vert}\left(\mathbf{R}_D^0\right)$	uncorrected	9.802	9.812	10.258	10.226
	corrected	9.842	9.852	10.297	10.265
$IP_{SD}^{vert}\left(\mathbf{R}_S^+\right)$	uncorrected	9.797	9.780	10.225	10.194
	corrected	9.836	9.819	10.265	10.233
IP_{SD}^{ad}	uncorrected	9.783	9.794	10.215	10.187
	corrected	9.823	9.833	10.254	10.227

Table S23: Values of the vertical and adiabatic doublet-singlet ionization energy ($IP_{SD}^{vert}(\mathbf{R}) \equiv \mathcal{E}_S^+(\mathbf{R}) - \mathcal{E}_D^0(\mathbf{R})$ and $IP_{SD}^{ad} \equiv \mathcal{E}_S^+\left(\mathbf{R}_S^+\right) - \mathcal{E}_D^0(\mathbf{R}_D^0)$, respectively) computed without and with corrections due to zero point motion using 6-311++G(3df, 3pd) basis sets and the neutral doublet ($\mathbf{R} = \mathbf{R}_D^0$) and cation singlet ($\mathbf{R} = \mathbf{R}_S^+$) geometries optimized within B3LYP/6-311++G(3df, 3pd) and PBE0/6-311++G(3df, 3pd).

		B3LYP	PBE0	EOM-ROCCSD@B3LYP	EOM-ROCCSD@PBE0
$IP_{SD}^{vert}(\mathbf{R}_D^0)$	uncorrected	9.812	9.874	9.802	9.805
	corrected	9.852	9.915	9.842	9.845
$IP_{SD}^{vert}\left(\mathbf{R}_S^+\right)$	uncorrected	9.780	9.844	9.797	9.801
	corrected	9.819	9.884	9.836	9.841
IP_{SD}^{ad}	uncorrected	9.794	9.857	9.783	9.800
	corrected	9.833	9.897	9.823	9.840

Table S24: Values of the vertical and adiabatic doublet-singlet ionization energy IP computed without and with corrections due to zero point motion using the neutral doublet $\mathbf{R}_D^0$ and cation singlet $\mathbf{R}_S^+$ geometries optimized by means of several functionals and 6-311++G(3df, 3pd) basis sets.

		B3LYP	PBE0	M06-2X
$IP_{SD}^{vert}(\mathbf{R}_D^0)$	uncorrected	9.812	9.874	9.835
	corrected	9.852	9.915	9.946
$IP_{SD}^{vert}\left(\mathbf{R}_S^+\right)$	uncorrected	9.780	9.844	9.812
	corrected	9.819	9.884	9.822
IP_{SD}^{ad}	uncorrected	9.794	9.857	9.822
	corrected	9.833	9.897	9.832

Table S25: Quadrupole moment **Q** (field independent basis, debye-angstrom) of the isoelectronic C_4N^- and HC_4N chains computed as indicated in the second column.

Species	Method	Q_{xx}	Q_{yy}	Q_{zz}	Q_{xy}	Q_{xz}	Q_{yz}
C_4N^- triplet	B3LYP/6-311++G(3df, 3pd)	-34.2070	-68.9571	-31.7034	-9.6536	0.0000	0.0000
	B3LYP/aug-cc-pVTZ	-34.1971	-69.0040	-31.6890	-9.6702	0.0000	0.0000
	UCCSD(T)/6-311++G(3df, 3pd)	-34.3255	-69.2273	-31.8029	-9.7128	0.0000	0.0000
	ROCCSD(T)/6-311++G(3df, 3pd)	-34.5067	-67.8347	-32.1155	-9.2375	0.0000	0.0000
	ROCCSD(T)/aug-cc-pVTZ	-34.4814	-67.8801	-32.0848	-9.2581	0.0000	0.0000
HC_4N triplet	B3LYP/6-311++G(3df, 3pd)	-28.4399	-27.7588	-28.4371	-0.1693	0.0000	0.0000
	B3LYP/aug-cc-pVTZ	-28.4196	-27.7593	-28.4116	-0.1574	0.0000	0.0000
	UCCSD(T)/6-311++G(3df, 3pd)	-28.4547	-27.4563	-28.5638	-0.3883	0.0000	0.0000
	ROCCSD(T)/6-311++G(3df, 3pd)	-29.0226	-28.2790	-29.0194	-0.1844	0.0000	0.0000
	ROCCSD(T)/aug-cc-pVTZ	-28.9932	-28.2743	-28.9830	-0.1694	0.0000	0.0000
bent C_4N^- singlet	B3LYP/6-311++G(3df, 3pd)	-63.8640	-36.8339	-30.3058	1.4754	0.0001	0.0001
	B3LYP/aug-cc-pVTZ	-63.8640	-36.8339	-30.3058	1.4754	0.0001	0.0001
	RCCSD(T)/6-311++G(3df, 3pd)	-62.9911	-37.1863	-30.6481	1.1594	0.0000	0.0001
	RCCSD(T)/aug-cc-pVTZ	-63.0000	-37.1600	-30.6336	1.1690	0.0001	0.0001
HC_4N singlet	B3LYP/6-311++G(3df, 3pd)	-27.3591	-30.3776	-27.1872	-4.3257	0.0000	0.0000
	B3LYP/aug-cc-pVTZ	-27.3407	-30.3437	-27.1738	-4.3184	0.0000	0.0000
	RCCSD(T)/6-311++G(3df, 3pd)	-27.1081	-30.8650	-27.7089	-4.6705	0.0000	0.0000
	RCCSD(T)/aug-cc-pVTZ	-27.0845	-30.8217	-27.6860	-4.6599	0.0000	0.0000

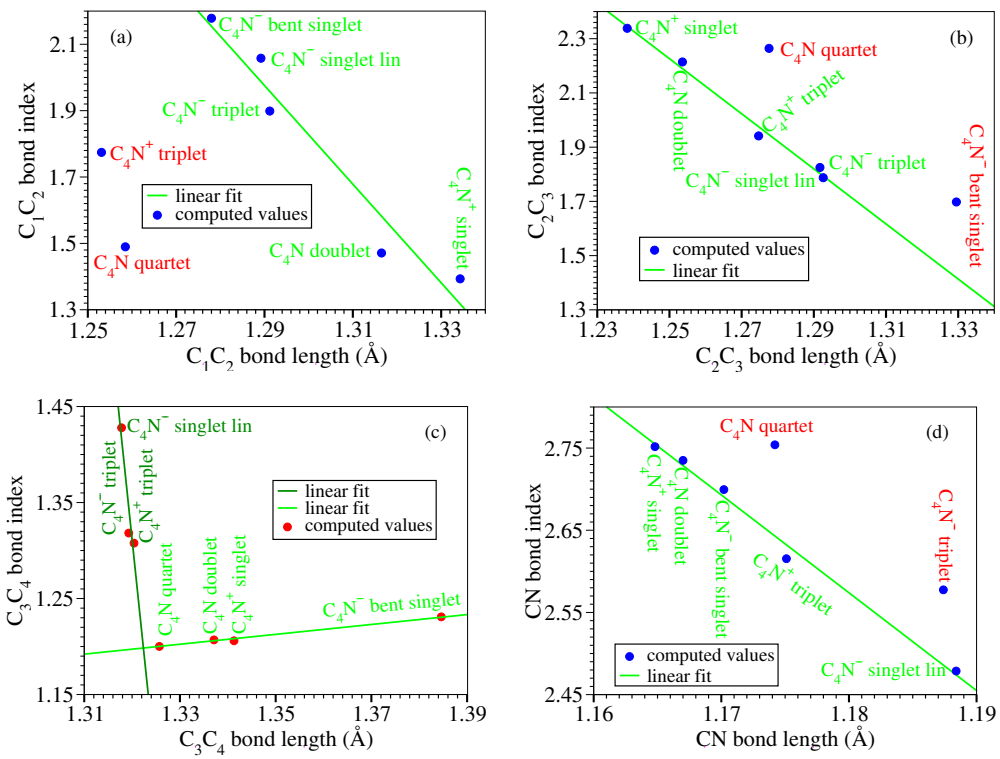

Figure S20: Bond order indices versus bond lengths of the C_4N chains investigated in the present paper. The linear fitting line suggests possible correlations.

Table S26: Reorganization energies $\lambda_a^b \equiv \mathcal{E}_a(\mathbf{R}_b) - \mathcal{E}_a(\mathbf{R}_a)$ of the C_4N anions — triplet (T^-), bent singlet (bS^-) and (metastable) linear singlet (lS^-) — with respect to the neutral doublet (D).

Functional	$\lambda_{T^-}^{D}$	$\lambda_{D}^{T^-}$	$\lambda_{bS^-}^{D}$	$\lambda_{D}^{bS^-}$	$\lambda_{lS^-}^{D}$	$\lambda_{D}^{lS^-}$
B3LYP	0.067	0.076	0.338	0.488	0.082	0.081
PBE0	0.067	0.076	0.342	0.509	0.087	0.087
M06-2X	0.081	-0.113	0.446	0.600	0.111	0.110

Table S27: Reorganization energies $\lambda_a^b \equiv \mathcal{E}_a(\mathbf{R}_b) - \mathcal{E}_a(\mathbf{R}_a)$ of the C_4N singlet (S^+) and triplet (T^+) cations with respect to the neutral doublet (D).

Functional	$\lambda_{S^+}^{D}$	$\lambda_{D}^{S^+}$	$\lambda_{T^+}^{D}$	$\lambda_{D}^{T^+}$
B3LYP	0.019	0.014	0.124	0.124
PBE0	0.018	0.013	0.121	0.121
M06-2X	0.014	0.010	0.138	0.138

Table S28: Dissociation of neutral and anion C_4N chains. Enthalpies of reaction at zero (subscript 0) and room temperature (subscript RT) computed by several CBS protocols.[24] All values (in kcal/mol) refer to the electronic ground states.

No.	Species	Method		Reaction				$\Delta_r H_0^0$	$\Delta_r H_{RT}^0$
1	C_4N	C_4N	$\rightarrow$	C	+	C_3N	CBS-QB3	139.4	140.1
		C_4N	$\rightarrow$	C	+	C_3N	CBS-APNO	137.3	138.0
		C_4N	$\rightarrow$	C	+	C_3N	CBS-4M	138.6	139.6
2		C_4N	$\rightarrow$	C_2	+	C_2N	CBS-QB3	152.0	152.8
		C_4N	$\rightarrow$	C_2	+	C_2N	CBS-APNO	152.0	155.9
		C_4N	$\rightarrow$	C_2	+	C_2N	CBS-4M	155.2	156.3
3		C_4N	$\rightarrow$	C_3	+	CN	CBS-QB3	95.3	96.4
		C_4N	$\rightarrow$	C_3	+	CN	CBS-APNO	94.2	95.3
		C_4N	$\rightarrow$	C_3	+	CN	CBS-4M	103.0	104.3
4		C_4N	$\rightarrow$	C_4	+	N	CBS-QB3	159.6	160.5
		C_4N	$\rightarrow$	C_4	+	N	CBS-APNO	157.8	158.5
		C_4N	$\rightarrow$	C_4	+	N	CBS-4M	156.6	157.7
5a	C_4N^-	C_4N^-	$\rightarrow$	C	+	C_3N^-	CBS-QB3	109.1	109.4
		C_4N^-	$\rightarrow$	C	+	C_3N^-	CBS-APNO	110.8	111.6
		C_4N^-	$\rightarrow$	C	+	C_3N^-	CBS-4M	116.6	117.5
5b		C_4N^-	$\rightarrow$	C^-	+	C_3N	CBS-QB3	184.4	185.4
		C_4N^-	$\rightarrow$	C^-	+	C_3N	CBS-APNO	183.9	184.8
		C_4N^-	$\rightarrow$	C^-	+	C_3N	CBS-4M	190.9	191.8
6a		C_4N^-	$\rightarrow$	C_2	+	C_2N^-	CBS-QB3	160.6	161.6
		C_4N^-	$\rightarrow$	C_2	+	C_2N^-	CBS-APNO	166.2	170.0
		C_4N^-	$\rightarrow$	C_2	+	C_2N^-	CBS-4M	165.5	166.6
6b		C_4N^-	$\rightarrow$	C_2^-	+	C_2N	CBS-QB3	151.0	152.1
		C_4N^-	$\rightarrow$	C_2^-	+	C_2N	CBS-APNO	152.6	153.5
		C_4N^-	$\rightarrow$	C_2^-	+	C_2N	CBS-4M	156.9	158.0
7a		C_4N^-	$\rightarrow$	C_3	+	CN^-	CBS-QB3	77.6	79.0
		C_4N^-	$\rightarrow$	C_3	+	CN^-	CBS-APNO	79.7	81.0
		C_4N^-	$\rightarrow$	C_3	+	CN^-	CBS-4M	88.4	89.7
7b		C_4N^-	$\rightarrow$	C_3^-	+	CN	CBS-QB3	122.0	123.3
		C_4N^-	$\rightarrow$	C_3^-	+	CN	CBS-APNO	122.4	123.4
		C_4N^-	$\rightarrow$	C_3^-	+	CN	CBS-4M	130.2	131.5
8a		C_4N^-	$\rightarrow$	C_4	+	N^-	CBS-QB3	238.1	239.4
		C_4N^-	$\rightarrow$	C_4	+	N^-	CBS-APNO	241.8	243.0
		C_4N^-	$\rightarrow$	C_4	+	N^-	CBS-4M	241.8	243.0
8b		C_4N^-	$\rightarrow$	C_4^-	+	N	CBS-QB3	141.8	142.8
		C_4N^-	$\rightarrow$	C_4^-	+	N	CBS-APNO	142.5	143.3
		C_4N^-	$\rightarrow$	C_4^-	+	N	CBS-4M	144.6	145.8

Table S29: Dissociation of neutral C_2N, C_3N, and C_5N chains already detected in space. Enthalpies of reaction at zero (subscript 0) and room temperature (subscript RT) computed by several CBS protocols.[24] All values (in kcal/mol) refer to the electronic ground states.

No.	Species	Reaction					Method	$\Delta_r H_0^0$	$\Delta_r H_{RT}^0$
9a	C_2N	C_2N	$\rightarrow$	C	+	CN	CBS-QB3	113.4	114.4
		C_2N	$\rightarrow$	C	+	CN	CBS-APNO	113.1	114.1
		C_2N	$\rightarrow$	C	+	CN	CBS-4M	116.6	117.7
9b		C_2N	$\rightarrow$	C_2	+	N	CBS-QB3	145.8	146.8
		C_2N	$\rightarrow$	C_2	+	N	CBS-APNO	149.3	148.7
		C_2N	$\rightarrow$	C_2	+	N	CBS-4M	147.5	148.7
10a	C_3N	C_3N	$\rightarrow$	C	+	C_2N	CBS-QB3	156.8	157.9
		C_3N	$\rightarrow$	C	+	C_2N	CBS-APNO	158.8	159.7
		C_3N	$\rightarrow$	C	+	C_2N	CBS-4M	158.0	159.0
10b		C_3N	$\rightarrow$	C_2	+	CN	CBS-QB3	126.0	127.1
		C_3N	$\rightarrow$	C_2	+	CN	CBS-APNO	131.0	132.0
		C_3N	$\rightarrow$	C_2	+	CN	CBS-4M	133.2	134.4
10c		C_3N	$\rightarrow$	C_3	+	N	CBS-QB3	132.6	134.0
		C_3N	$\rightarrow$	C_3	+	N	CBS-APNO	133.9	135.2
		C_3N	$\rightarrow$	C_3	+	N	CBS-4M	136.7	138.0
12a	C_5N	C_5N	$\rightarrow$	C	+	C_4N	CBS-QB3	144.1	145.7
		C_5N	$\rightarrow$	C	+	C_4N	CBS-APNO	147.2	148.1
		C_5N	$\rightarrow$	C	+	C_4N	CBS-4M	147.3	148.2
12b		C_5N	$\rightarrow$	C_2	+	C_3N	CBS-QB3	139.2	140.6
		C_5N	$\rightarrow$	C_2	+	C_3N	CBS-APNO	143.7	144.3
		C_5N	$\rightarrow$	C_2	+	C_3N	CBS-4M	144.6	145.5
12c		C_5N	$\rightarrow$	C_3	+	C_2N	CBS-QB3	126.0	127.8
		C_5N	$\rightarrow$	C_3	+	C_2N	CBS-APNO	128.3	129.3
		C_5N	$\rightarrow$	C_3	+	C_2N	CBS-4M	133.7	134.8
12d		C_5N	$\rightarrow$	C_4	+	CN	CBS-QB3	126.9	128.6
		C_5N	$\rightarrow$	C_4	+	CN	CBS-APNO	128.0	128.7
		C_5N	$\rightarrow$	C_4	+	CN	CBS-4M	131.6	132.7
12e		C_5N	$\rightarrow$	C_5	+	N	CBS-QB3	135.8	137.3
		C_5N	$\rightarrow$	C_5	+	N	CBS-APNO	136.0	136.8
		C_5N	$\rightarrow$	C_5	+	N	CBS-4M	142.9	143.8

Table S30: Relevant exchange reactions. Enthalpies of reaction at zero (subscript 0) and room temperature (subscript RT) computed by several CBS protocols.[24] All values (in kcal/mol) refer to the electronic ground states.

No.	Reaction							Method	$\Delta_r H_0^0$	$\Delta_r H_{RT}^0$
13	C_5	+	N	→	C	+	C_4N	CBS-QB3	8.3	8.4
	C_5	+	N	→	C	+	C_4N	CBS-APNO	11.2	11.3
	C_5	+	N	→	C	+	C_4N	CBS-4M	4.5	4.3
14a	N	+	C_4H^-	→	C_4N	+	H^-	CBS-QB3	23.9	24.3
	N	+	C_4H^-	→	C_4N	+	H^-	CBS-APNO	32.2	32.9
	N	+	C_4H^-	→	C_4N	+	H^-	CBS-4M	24.3	24.6
14b	N	+	C_4H^-	→	C_4N^-	+	H	CBS-QB3	-36.0	-35.9
	N	+	C_4H^-	→	C_4N^-	+	H	CBS-APNO	-36.6	-36.1
	N	+	C_4H^-	→	C_4N^-	+	H	CBS-4M	-41.6	-41.3
14c	N^-	+	C_4H	→	C_4N^-	+	H	CBS-QB3	-125.0	-124.8
	N^-	+	C_4H	→	C_4N^-	+	H	CBS-APNO	-137.1	-136.9
	N^-	+	C_4H	→	C_4N^-	+	H	CBS-4M	-129.2	-129.2
14d	N^-	+	C_4H	→	C_4N	+	H^-	CBS-QB3	-65.1	-64.6
	N^-	+	C_4H	→	C_4N	+	H^-	CBS-APNO	-68.3	-67.9
	N^-	+	C_4H	→	C_4N	+	H^-	CBS-4M	-63.3	-63.3
15a	CN	+	C_3H	→	H	+	C_4N	CBS-QB3	-20.5	-20.4
	CN	+	C_3H	→	H	+	C_4N	CBS-APNO	-18.9	-18.9
	CN	+	C_3H	→	H	+	C_4N	CBS-4M	-24.8	-24.8
15b	CN^-	+	C_3H	→	H	+	C_4N^-	CBS-QB3	-2.8	-3.0
	CN^-	+	C_3H	→	H	+	C_4N^-	CBS-APNO	-4.5	-4.6
	CN^-	+	C_3H	→	H	+	C_4N^-	CBS-4M	-10.2	-10.2
15c	CN^-	+	C_3H	→	H^-	+	C_4N	CBS-QB3	57.1	57.2
	CN^-	+	C_3H	→	H^-	+	C_4N	CBS-APNO	64.4	64.4
	CN^-	+	C_3H	→	H^-	+	C_4N	CBS-4M	55.7	55.8
15d	CN	+	C_3H^-	→	H	+	C_4N^-	CBS-QB3	-50.9	-50.8
	CN	+	C_3H^-	→	H	+	C_4N^-	CBS-APNO	-51.9	-51.6
	CN	+	C_3H^-	→	H	+	C_4N^-	CBS-4M	-56.7	-56.8
15e	CN	+	C_3H^-	→	H^-	+	C_4N	CBS-QB3	9.0	9.4
	CN	+	C_3H^-	→	H^-	+	C_4N	CBS-APNO	16.9	17.4
	CN	+	C_3H^-	→	H^-	+	C_4N	CBS-4M	9.2	9.2

Table S31: Relevant exchange reactions. Enthalpies of reaction at zero (subscript 0) and room temperature (subscript RT) computed by several CBS protocols.[24] All values (in kcal/mol) refer to the electronic ground states.

No.	Reaction							Method	$\Delta_r H_0^0$	$\Delta_r H_{RT}^0$
16a	CH	+	C_3N	→	H	+	C_4N	CBS-QB3	-59.4	-59.2
	CH	+	C_3N	→	H	+	C_4N	CBS-APNO	-57.4	-57.2
	CH	+	C_3N	→	H	+	C_4N	CBS-4M	-58.9	-58.9
16b	CH^-	+	C_3N	→	H	+	C_4N^-	CBS-QB3	-105.6	-105.8
	CH^-	+	C_3N	→	H	+	C_4N^-	CBS-APNO	-105.0	-105.0
	CH^-	+	C_3N	→	H	+	C_4N^-	CBS-4M	-111.0	-111.1
16c	CH^-	+	C_3N	→	H^-	+	C_4N	CBS-QB3	-45.8	-45.5
	CH^-	+	C_3N	→	H^-	+	C_4N	CBS-APNO	-36.2	-36.0
	CH^-	+	C_3N	→	H^-	+	C_4N	CBS-4M	-45.1	-45.2
16d	CH	+	C_3N^-	→	H	+	C_4N^-	CBS-QB3	-29.1	-29.1
	CH	+	C_3N^-	→	H	+	C_4N^-	CBS-APNO	-31.0	-30.8
	CH	+	C_3N^-	→	H	+	C_4N^-	CBS-4M	-36.8	-36.9
17a	CH	+	C_3N^-	→	H^-	+	C_4N	CBS-QB3	30.8	31.1
	CH	+	C_3N^-	→	H^-	+	C_4N	CBS-APNO	37.9	38.2
	CH	+	C_3N^-	→	H^-	+	C_4N	CBS-4M	29.1	29.1
17b	C_2H	+	C_2N	→	H	+	C_4N	CBS-QB3	-40.4	-40.3
	C_2H	+	C_2N	→	H	+	C_4N	CBS-APNO	-41.0	-40.5
	C_2H	+	C_2N	→	H	+	C_4N	CBS-4M	-40.4	-40.3
17c	C_2H^-	+	C_2N	→	H	+	C_4N^-	CBS-QB3	-44.6	-44.5
	C_2H^-	+	C_2N	→	H	+	C_4N^-	CBS-APNO	-46.6	-46.2
	C_2H^-	+	C_2N	→	H	+	C_4N^-	CBS-4M	-51.7	-51.5
17d	C_2H^-	+	C_2N	→	H^-	+	C_4N	CBS-QB3	15.3	15.7
	C_2H^-	+	C_2N	→	H^-	+	C_4N	CBS-APNO	22.2	22.8
	C_2H^-	+	C_2N	→	H^-	+	C_4N	CBS-4M	14.2	14.5
17e	C_2H	+	C_2N^-	→	H^-	+	C_4N	CBS-QB3	10.8	11.2
	C_2H	+	C_2N^-	→	H^-	+	C_4N	CBS-APNO	16.8	17.5
	C_2H	+	C_2N^-	→	H^-	+	C_4N	CBS-4M	15.1	15.3
17f	C_2H	+	C_2N^-	→	H	+	C_4N^-	CBS-QB3	-49.1	-49.0
	C_2H	+	C_2N^-	→	H	+	C_4N^-	CBS-APNO	-52.0	-51.5
	C_2H	+	C_2N^-	→	H	+	C_4N^-	CBS-4M	-50.8	-50.6

Table S32: Relevant exchange reactions. Enthalpies of reaction at zero (subscript 0) and room temperature (subscript RT) computed by several CBS protocols.[24] All values (in kcal/mol) refer to the electronic ground states.

No.	Reaction							Method	$\Delta_r H_0^0$	$\Delta_r H_{RT}^0$
18	NC_2N	+	C_2	$\rightarrow$	N	+	C_4N	CBS-QB3	48.6	49.0
	NC_2N	+	C_2	$\rightarrow$	N	+	C_4N	CBS-APNO	45.2	45.6
	NC_2N	+	C_2	$\rightarrow$	N	+	C_4N	CBS-4M	41.4	41.5
19	NC_2N	+	C_2N	$\rightarrow$	N_2	+	C_4N	CBS-QB3	-29.8	-29.3
	NC_2N	+	C_2N	$\rightarrow$	N_2	+	C_4N	CBS-APNO	-29.4	-28.9
	NC_2N	+	C_2N	$\rightarrow$	N_2	+	C_4N	CBS-4M	-31.7	-31.4
20	NC_2N	+	C_2H	$\rightarrow$	NH	+	C_4N	CBS-QB3	82.3	82.7
	NC_2N	+	C_2H	$\rightarrow$	NH	+	C_4N	CBS-APNO	81.4	82.2
	NC_2N	+	C_2H	$\rightarrow$	NH	+	C_4N	CBS-4M	78.0	78.4

Table S33: Adiabatic electron affinities and ionization potentials (in eV) of C_4N and C_6N computed with various CBS protocols. Notice that, out of these protocols, the CBS-QB3 EA-estimates are the closest to the experimental values $EA_{C_2N} = 2.74890 \pm 0.00010\,\text{eV}$, $EA_{C_4N} = 3.1113 \pm 0.00010\,\text{eV}$ and $EA_{C_4N} = 3.3715 \pm 0.00010\,\text{eV}$.[20]

Method	EA_{C_2N}	IP_{C_2N}	EA_{C_4N}	IP_{C_4N}	EA_{C_6N}	IP_{C_6N}
CBS-QB3	2.7615	10.8166	3.1351	9.6913	3.4804	8.9994
CBS-APNO	2.7728	10.8178	3.2506	9.6332	3.5648	8.9491
CBS-4M	3.0115	11.1315	3.4596	10.0462	3.7693	9.5614